

Antiferromagnetic order with short correlation length and Kondo interactions in U_2PdGa_3 and U_2PtGa_3

V. H. Tran

*Max-Planck Institute for Chemical Physics of Solids, D-01187 Dresden, Germany**and W. Trzebiatowski Institute of Low Temperature and Structure Research, Polish Academy of Sciences, 50-950 Wrocław, Poland*

F. Steglich

Max-Planck Institute for Chemical Physics of Solids, D-01187 Dresden, Germany

G. André

Laboratoire Léon Brillouin, (CEA-CNRS), CEA/Saclay, 91191 Gif-Sur-Yvette Cedex, France

(Received 22 January 2001; revised manuscript received 27 November 2001; published 8 March 2002)

We report the results of magnetic susceptibility, magnetoresistance, specific heat, and neutron-powder-diffraction measurements on U_2PdGa_3 and U_2PtGa_3 . The investigated compounds crystallize in the orthorhombic $CeCu_2$ -type structure (space group $Imma$) and, at $T_N \approx 30$ K, undergo an antiferromagnetic state with finite magnetic correlation lengths 120–150 Å. The magnetic structure is collinear and with the uranium magnetic moments aligned parallel to the orthorhombic c axis. At 1.4 K, the uranium magnetic moments are estimated to be about $(0.3-0.4)\mu_B/U$. Despite showing the signature of three-dimensional almost long-range antiferromagnetic order below 30 K in the dc-magnetic susceptibility, for both compounds a discontinuity in the specific heat at their Néel temperatures is lacking. Furthermore, the dc-magnetic susceptibility displays magnetic-history phenomena, while the magnetoresistance data indicate the existence of Kondo interactions in the magnetically ordered state. We discuss the observed magnetic behavior in terms of a competition between randomness, Kondo and magnetic exchange interactions.

DOI: 10.1103/PhysRevB.65.134401

PACS number(s): 75.20.Hr, 75.25.+z

I. INTRODUCTION

In previous work we investigated the uranium-based intermetallic compounds U_2TGa_3 , where $T = Ru, Rh, Pd, Ir$, and Pt .¹ We found that these compounds crystallize in an orthorhombic $CeCu_2$ -type structure (space group $Imma$). Based on magnetization, magnetic-susceptibility, and electrical-resistivity data, we found that the ground states of U_2RuGa_3 , U_2RhGa_3 , and U_2IrGa_3 are ferromagnetic, while both U_2PdGa_3 and U_2PtGa_3 undergo an antiferromagnetic (AF) ordering below 30 and 33 K, respectively. In addition, a ferromagnetic-phase-transition anomaly occurs in both ac and dc susceptibilities at $T_m = 80$ K for the latter compound.

Moreover, inspecting the compounds of the related U_2TSi_3 family, one observes either long-range ferromagnetic order^{2,3} or spin-glass (SG) freezing.⁴⁻⁷ The occurrence of a spin-glass state in some U_2TSi_3 compounds is believed to originate from the randomly frustrated U-U interactions resulting from atomic disorder inherent to an $A1B_2$ -type crystal lattice.

These results make U_2TGa_3 compounds interesting materials for a thorough investigation, as one expects, that owing to the existence of the magnetic order, strong U-U magnetic exchange interactions overcome magnetic fluctuations due to the randomness. In the present paper, our results for magnetization, magnetoresistance, specific-heat, and neutron-powder-diffraction measurements on the two antiferromagnets U_2PdGa_3 and U_2PtGa_3 will be presented.

II. EXPERIMENTAL DETAILS

Polycrystalline samples of about 10 g for U_2PdGa_3 and U_2PtGa_3 were prepared by arc melting using a procedure

previously described.¹ The characterization of the samples by x-ray powder diffraction was performed at room temperature. The U_2PdGa_3 sample was found to be of single phase. In the case of U_2PtGa_3 , in addition to the major phase of the orthorhombic $CeCu_2$ -type crystal structure, a small amount of impurity phases (less than 3% in mass) was detected. However, by means of neutron-diffraction measurement we found that the contamination is on a somewhat higher level. We have identified the main impurity phase as UGa_3 , which appears to be less than 3% in U_2PdGa_3 and about 7% in the case of U_2PtGa_3 . As we will show below, any anomaly of such kind of order due to the impurity UGa_3 ($T_N = 70$ K) was not observed in our data. The calculated lattice parameters based on the Bragg reflections of the major phase were consistent with previously reported data.¹

The dc-magnetic susceptibility $\chi(T) = M/H$ was measured by means of a superconducting quantum-interference-device magnetometer (Quantum Design MPMS-5) in fields H up to 50 kOe and in a temperature range of 2–100 K. These measurements were carried out in each case on three different pieces of the sample. The fact that we obtained identical results for the three pieces rules out significant macroscopic inhomogeneities in our samples. The absolute accuracy in $\chi(T)$ is of about 5%, limited partly by a demagnetizing factor, which was not taken into account in data analysis. A large contribution to this experimental error arises from a large magnetocrystalline anisotropy and from some texture effect existing in the samples. The dc-magnetization measurements in fields up to 140 kOe at several temperatures below 60 K and ac-magnetic susceptibility

measurements in a frequency range of 30–1000 Hz were performed using a Quantum Design PPMS. The amplitude of the oscillating frequency was $H_{ac} = 10$ Oe.

The electrical resistivity $\rho(T)$ was measured in a Quantum Design PPMS, using a four-probe ac technique in a temperature range of 1.8–300 K. The samples were rectangular with typical dimensions $0.5 \times 0.5 \times 5$ mm³. A current of 5 mA at a frequency of 37 Hz was supplied to the samples. The resistivity in a fixed magnetic field of $H = 100$ kOe was measured on zero-field-cooled samples in a temperature range of 1.8–120 K. The resistivity data were also collected in fields up to 140 kOe at several selected temperatures below 100 K. The magnetoresistance is defined as $\Delta\rho/\rho = [\rho(T, H) - \rho(T, 0)]/\rho(T, 0)$. The magnetic fields were applied perpendicular to the direction of the current. The experimental error in the resistivity is less than 5%, due mainly to the uncertainty in the geometrical factor.

The specific heat $C_p(T)$ measurements were performed in a Quantum Design PPMS in a temperature range of 1.8–240 K, utilizing a relaxation method.

Neutron-powder-diffraction (NPD) experiments were performed on the G4.1 diffractometer ($\lambda = 2.426$ Å) installed at the Orphée reactor in Laboratoire Léon Brillouin, Saclay. The diffraction patterns were collected at several temperatures in the range 1.4–90 K. The experimental neutron-diffraction data were analyzed by the Rietveld profile fitting method using the FULLPROF program,⁸ based on the nuclear scattering lengths published by Sears.⁹ In the magnetic refinements, we used the magnetic form factor of U^{3+} calculated in the dipolar approximation by Freeman *et al.*¹⁰

III. RESULTS AND DISCUSSION

A. Structural properties

The NPD patterns obtained at 40 K for U_2PdGa_3 and 90 K for U_2PtGa_3 (Fig. 1) show nuclear reflections corresponding to an orthorhombic $CeCu_2$ -type structure. In the crystal-structure refinement, we have applied a peak-shape function of pseudo-Voigt type to all the reflections. The refinement ends at the reasonable agreement values $R_B = 3.9\%$ for the Pd-based compound and 6.2% for the Pt-based compound, respectively. Thus, by means of NPD, we confirm an orthorhombic $CeCu_2$ -type structure with the space group $Imma$ for both U_2PdGa_3 and U_2PtGa_3 . The fitting results are shown as solid lines in Fig. 1 and listed in Table I.

In a $CeCu_2$ -type structure, the uranium atoms occupy the four equivalent positions ($4e$), while the transition-metal and gallium atoms are randomly distributed in eight equivalent positions ($8h$). Owing to the mixed site occupation of the transition-metal and gallium atoms, we have checked possible atomic short-range order, applying the peak-shape function of Thompson-Cox-Hastings pseudo-Voigt type in the calculation. We estimated a correlation length ξ , based on the inverse of the full width at half maximum of the nuclear peaks. We obtained a value of ξ of about 1300 Å for both compounds, indicating that the atoms have a true long-range correlation. As we will discuss below, the atomic disorder may nevertheless give rise to some randomness in the U-U

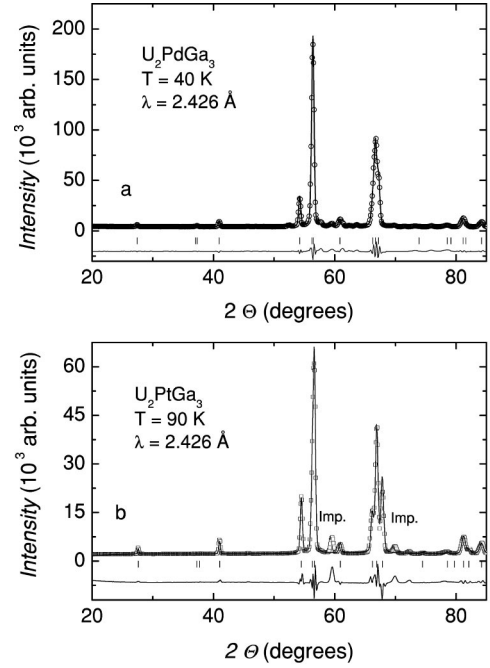


FIG. 1. Neutron-diffraction patterns of (a) U_2PdGa_3 and (b) U_2PtGa_3 at 40 and 90 K, respectively. Open points represent the measured data points, and solid lines show the calculated profiles. The difference between measured and calculated profiles is plotted on the lower scale.

exchange interactions and, thus, provides a significant influence on the observed magnetic properties.

We have calculated the values of the shortest distances between the four uranium atoms: $U1(0, 1/4, z_U)$, $U2(0, 3/4, -z_U)$, $U3(1/2, 3/4, 1/2 + z_U)$, and $U4(1/2, 1/4, 1/2 - z_U)$. We distinguish between three nearest U-U distances (see Table I); the first one is the zigzag distances along the b axis, $d1_{U-U}$, the second one is between neighboring uranium atoms lying in two adjacent bc planes, i.e., along the a axis, $d2_{U-U}$; and the third one is identical to the lattice parameter a . For both compounds, $d1_{U-U} > d2_{U-U}$, which indicates that the nearest U neighbors form zigzag chains ($-U1-U2-U1-$ and $-U3-U4-U3-$) parallel to the b axis. The next-nearest U neighbors are connected by zigzag chains ($-U1-U4-U1-$ and $-U2-U3-U2-$) along the a axis. Upon decreasing the temperature, the lattice parameters of both compounds slightly

TABLE I. Crystallographic parameters of U_2PdGa_3 at 40 K and U_2PtGa_3 at 90 K.

	U_2PdGa_3	U_2PtGa_3
a (Å)	4.401(1)	4.381(1)
b (Å)	6.987(2)	7.021(2)
c (Å)	7.692(2)	7.713(2)
z_U	0.5346(5)	0.5404(10)
$y_{T/Ga}$	0.0385(5)	0.0420(16)
$z_{T/Ga}$	0.1663(13)	0.1641(31)
$d1_{U-U}$ (Å)	3.53	3.56
$d2_{U-U}$ (Å)	3.98	3.90

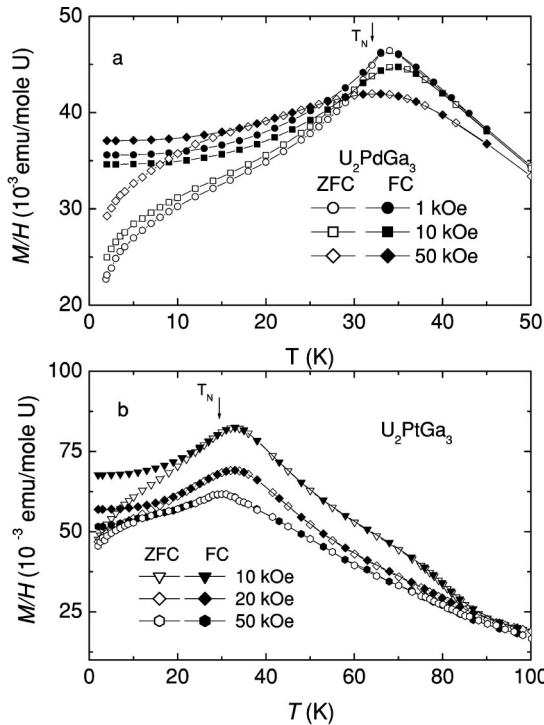


FIG. 2. Temperature dependence of the magnetic susceptibility $\chi(T)$ of (a) U_2PdGa_3 and (b) U_2PtGa_3 measured in zero-field-cooled and field-cooled modes for different magnetic fields. Arrows indicate Néel temperatures as determined by the maximum in $d(T\chi)/dT$.

decrease, whereas the atomic parameters are rather temperature independent in the covered temperature range.

B. Magnetic susceptibility

The results of the dc-magnetic susceptibility studies for U_2PdGa_3 are shown in Fig. 2(a). For small fields, the $\chi(T)$ curve exhibits a well-defined peak, arising from the AF phase transition. This peak is in agreement with previous observation.¹ An interesting result derives from comparing the temperature dependencies of the zero-field-cooled (ZFC) and field-cooled (FC) susceptibility: There is a difference between the ZFC and FC $\chi(T)$ curves below the Néel temperature T_N , defined as the position of the maximum in $\partial(T\chi)/\partial T$ (cf. arrows in Fig. 2). In particular, the temperature T_f , where ZFC and FC susceptibilities start to deviate, strongly depends on the strength of the magnetic field. In a low magnetic field, T_f almost coincides with the maximum of the magnetic susceptibility of 33 K, i.e., about 1.5° higher than T_N ; however in a field of 50 kOe, T_f amounts only to 17 K.

A similar irreversibility effect is also observed in the case of U_2PtGa_3 [Fig. 2(b)]. There exist differences between the two compounds: (i) an anomaly at about 80 K, which is suppressed in magnetic fields above 20 kOe, shows up for U_2PtGa_3 only and, for this compound; and (ii) the temperature T_f depends more strongly on H , being 14 K at $H = 50$ kOe.

The irreversibility of the magnetic susceptibility is a typical feature expected for spin glasses (SG's).^{11,12} Naturally,

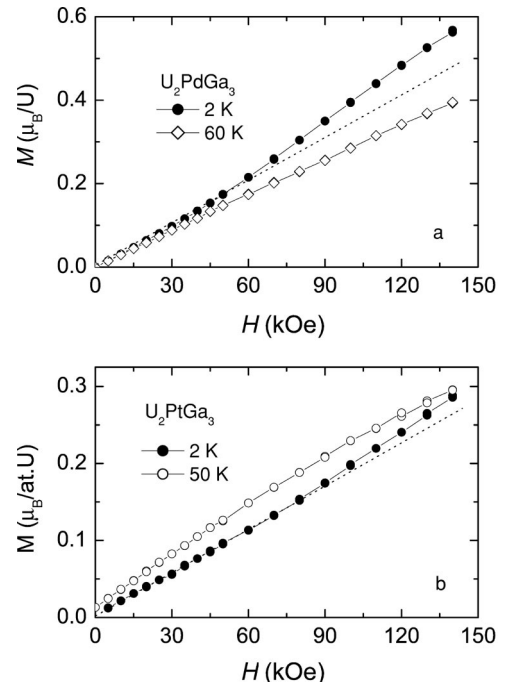


FIG. 3. (a) The magnetization M vs field for U_2PdGa_3 at 2 and 60 K. (b) The magnetization M vs field for U_2PtGa_3 at 2 and 50 K.

the disorder of Pd/Pt and Ga atoms in the crystal lattice may provide the random U-U exchange interaction necessary for the formation of the SG state. However, traditionally the SG state requires both disorder and frustration.^{11,12} A disordered $CeCu_2$ -type crystal structure (lacking any triangular or *kagome* lattices) cannot explain the occurrence of frustration. Hence it is not clear whether the irreversibility of $\chi(T)$ really arises from the “freezing of uranium spins.” Alternatively, the feature of “magnetic-history phenomena” was known to show up in alloys with long-range ordering as well as to be due to ferromagnetic domain-wall pinning effects.^{2,3} The following observations do not support a spin-glass conjecture: For our samples we observe only a small decrease of T_N with increasing fields, i.e., T_N is reduced to 30 K for U_2PdGa_3 and to 29 K for U_2PtGa_3 by a field of 50 kOe. The fields also do not considerably affect the intensity of the χ maximum, considering the fact that in an applied field of 50 kOe the maximum loses an intensity of about 10% compared to that in 1 kOe. Therefore, the irreversibility effect observed in our samples might be interpreted in terms of short-range magnetic interactions dictated by disorder effects. In this context, we would like to add that irreversibility effects have been observed quite often in intermetallic R_2TSi_3 and U_2TSi_3 compounds. A set of data was recently reported for single crystals of Tb_2PdSi_3 by Majumdar *et al.*¹³

Figure 3(a) shows the magnetization vs the applied field for U_2PdGa_3 at two temperatures. At 2 K, the M vs H behavior is linear up to about 50 kOe. Above this field, the $M(H)$ curve exhibits a slight upward tilt, followed by a tendency to saturate in high fields. This feature is beginning in a field of ~ 140 kOe, the highest available in our magnetometer. Such a behavior is a hallmark of the metamagnetic transition, and it should be observed in antiferromagnetic sys-

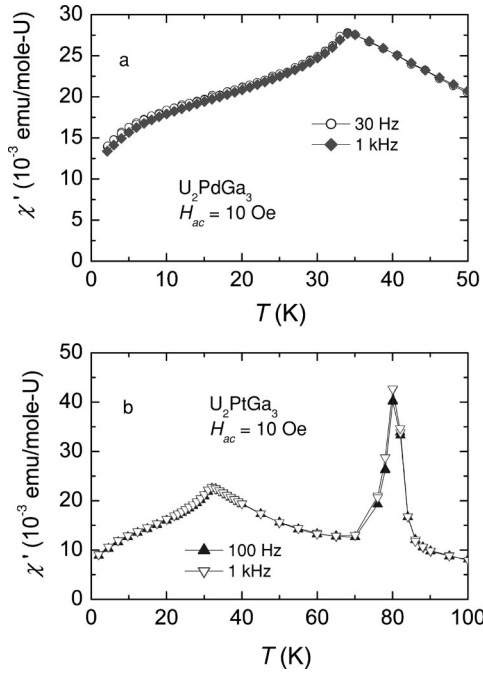


FIG. 4. (a) Temperature dependence of the ac-magnetic susceptibility of U_2PdGa_3 , measured at $H_{ac}=10$ Oe and at frequencies of 30 and 1000 Hz. (b) Temperature dependence of the ac-magnetic susceptibility of U_2PtGa_3 , measured at $H_{ac}=10$ Oe and at frequencies 100 and 1000 Hz.

tems. From the $1/M$ vs $1/H$ plot, a value of the uranium magnetic moment of $1.4\mu_B/at.U$ is obtained. At 60 K, the magnetization shows a monotonic change with fields, indicating a paramagnetic state of the compound.

In the case of U_2PtGa_3 [Fig. 3(b)], there is also a slight upward curvature, but at a field much higher than that for U_2PdGa_3 , i.e., of ~ 80 kOe. This behavior is consistent with the AF state of the compound. We recognize that the magnetization at 50 K shows a small spontaneous ferromagnetic moment, but complete saturation is not achieved even in 140 kOe.

Further, the AF ground state is more supported by the ac-magnetic susceptibility $\chi'(T)$ results shown in Fig. 4. $\chi'(T)$ clearly shows a sharp peak at 33.5 K for U_2PdGa_3 and at 31.8 K U_2PtGa_3 . The position of these peaks does not depend on the applied frequencies, at least up to 1 kHz. For U_2PtGa_3 we found another peak located around 80 K, which is of the ferromagnetic origin.

C. Electrical resistivity and magnetoresistance

In Fig. 5(a), we present the electrical-resistivity at zero field and 100 kOe as a function of temperature for U_2PdGa_3 . The zero-field resistivity in the high-temperature range (not shown) coincides with that previously reported:¹ it increases logarithmically with decreasing temperature. The resistivity keeps increasing down to 1.8 K, without any tendency toward a reduction which would signal the onset of coherence. The application of a magnetic field of 100 kOe leads to a depression of the electrical resistivity, i.e., to a negative magnetoresistance (MR). In single-ion Kondo systems, the MR is

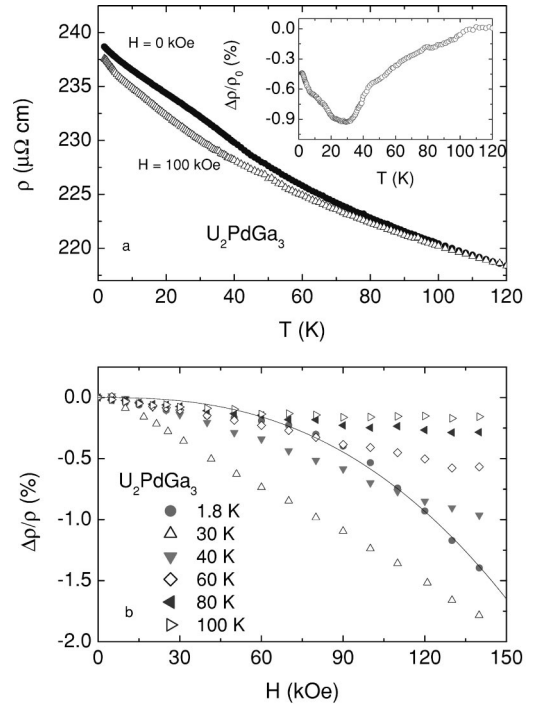


FIG. 5. (a) Temperature dependence of the electrical resistivity of U_2PdGa_3 , measured at zero and at a fixed magnetic field of 100 kOe. The inset shows the magnetoresistance obtained from the above data. (b) Isothermal magnetoresistance of U_2PdGa_3 as a function of the magnetic field. The solid line represents $\Delta\rho/\rho = aH^n$ ($n=2.6$), and is meant to be a fit to the $T=1.8$ K data.

negative at all temperatures due to the freezing out of spin-flip scattering by the magnetic field.¹⁴ In line with the Kondo-like behavior of the electrical resistivity at high temperatures,¹ this mechanism may also be operating in U_2PdGa_3 . A remarkable feature of our MR results, but rather common to magnetically ordered metals, is the occurrence of a minimum in $\Delta\rho/\rho$ vs T near T_N . Such a behavior is commonly understood as a significant suppression of spin fluctuations by the applied magnetic field. The MR of U_2PdGa_3 as a function of magnetic field is plotted in Fig. 5(b). For magnetic fields up to 140 kOe, the MR is negative in the range of measured temperatures. As long as the MR does not show any tendency to saturate, we believe that the uranium-derived magnetic moments do not tend to align ferromagnetically in the applied fields. In fact, the negative MR and the shape of $\Delta\rho/\rho$ vs H curves indicate the strong influence of Kondo interactions on the MR in the AF state. It is interesting to note that at temperatures below T_N , the MR varies as H^n with $n=2.6$. This behavior differs from that observed in SG systems, where $\Delta\rho/\rho$ also follows a power law H^n , but with $n\leq 2$.¹⁵

The temperature dependence of the electrical resistivity of U_2PtGa_3 is shown in Fig. 6(a). At zero field one observes a “knee” at $T_m=80$ K which is absent in the 100-kOe resistivity $\rho(100\text{ kOe}, T)$ data. Hence a deep minimum of the $\Delta\rho/\rho$ vs T curve develops around T_m , coinciding with T_m derived from the magnetic-susceptibility measurements [Fig. 2(b)]. The general behavior of the $\rho(T)$ curves taken at zero

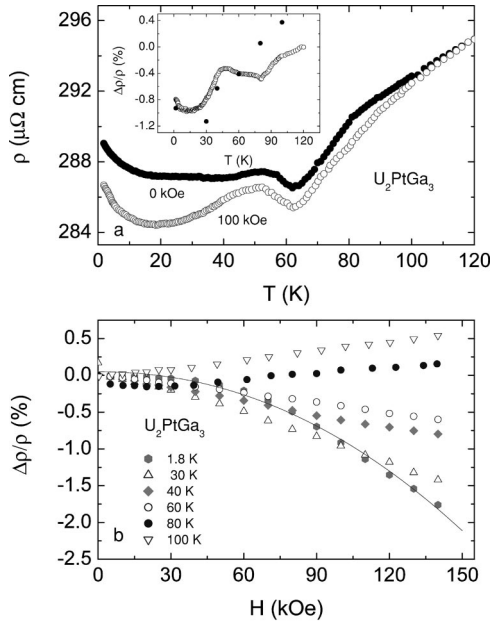


FIG. 6. (a) Temperature dependence of the electrical resistivity of U_2PtGa_3 , measured at zero field and at a fixed magnetic field of 100 kOe. The inset shows the magnetoresistance obtained from the above data and from those of (b) (full dots). (b) Isothermal magnetoresistance of U_2PtGa_3 as a function of the magnetic field. The solid line represents $\Delta\rho/\rho = aH^n$ ($n \approx 2.1$), and is meant to be a fit to the $T = 1.8$ K data.

field and 100 kOe is rather similar between 50 and 80 K, with a minimum in the resistivity at 60 K. Interestingly enough, such a minimum of $\rho(T)$ was already observed in the SG U_2PdSi_3 ,⁶ and in the re-entrant SG U_2RhSi_3 .⁷ For U_2PtGa_3 , the $\rho(T)$ minimum suggests two competing mechanisms: on the one hand, local Kondo interactions yielding an increase of the resistivity upon decreasing temperature, and on the other hand, the freezing out of spin-disorder scattering associated with magnetic short-range ordering. These different contributions to the MR yield different contributions to $\Delta\rho/\rho$ vs T in the presence of externally applied magnetic fields. This results in a large difference between the zero-field and 100-kOe curves below 50 K, displayed in Fig. 4(a). The fact that $\Delta\rho/\rho$ vs T does not exhibit another minimum at T_N , but rather at a temperature of 15 K, i.e., far below T_N , is surprising and calls for further studies.

The field dependence of the MR of U_2PtGa_3 [Fig. 6(b)] is somewhat different from that of U_2PdGa_3 [Fig. 5(b)]. For U_2PtGa_3 , we find a power-law behavior $\Delta\rho/\rho \propto H^n$ with $n \approx 2$, i.e., the exponent known for SG systems.¹⁵ It is clear that $\Delta\rho/\rho$ vs H changes sign near 80 K, i.e., becomes positive at higher T .

D. Specific heat

The results of the specific-heat, $C_p(T)$, measurements for U_2PdGa_3 are shown in Fig. 7. For the purpose of data analysis, the contributions to the specific heat are assumed to be additive. In the paramagnetic region, the total specific heat

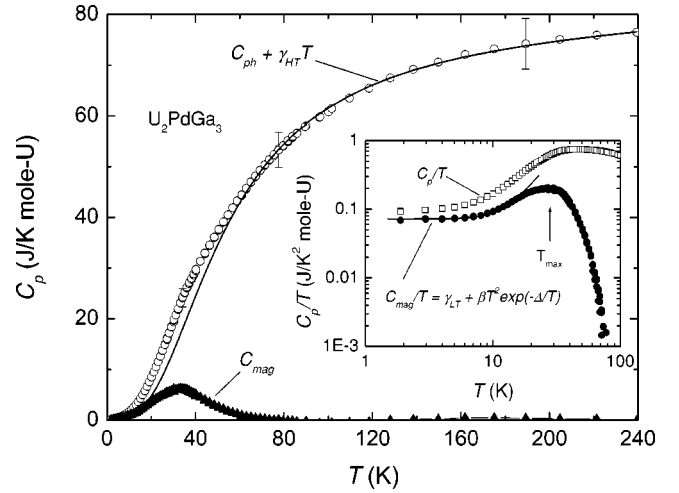


FIG. 7. Measured specific heat of U_2PdGa_3 (open circles), with an accuracy as indicated by the error bars, the sum of both the high-temperature electronic and phonon contributions (solid line), and the magnetic contribution (close triangles), as functions of temperature. Inset: the low-temperature part of the magnetic contribution and the raw C_p data in the C/T vs T representation. The solid line represents a fit to the low-temperature C_{mag} data (see the text).

C_p of U_2PdGa_3 consists of, at least, two distinct components: the lattice specific heat C_{ph} and the electronic specific heat C_{el} . The electronic contribution was taken as linearly temperature dependent, $C_{el}(T) = \gamma_{HT}T$. Owing to the lack of a suitable non- f -electron reference compound, we assumed $C_{ph}(T)$ of U_2PdGa_3 to be described by the Debye function, $C_{ph}(T) = 9R(T/\Theta_D)^3 \int_0^{\Theta_D/T} (x^4 e^x dx) / (e^x - 1)^2$. For temperatures between 70 and 240 K, the experimental data are then fit by the equation

$$C_p^*(T) = C_{ph}(T) + C_{el}(T), \quad (1)$$

with a Debye temperature $\Theta_D = 219(2)$ K and a Sommerfeld coefficient $\gamma_{HT} = 0.019(1)$ J/K² mole U. These values are typical for ternary uranium-based intermetallics. The Debye model works well at low temperatures ($T < \Theta_D/50$), but also for $T > \Theta_D/2$. In the intermediate temperature regime, it must be considered a very crude approximation to the phonon specific heat as measured. In Fig. 7 we also show the temperature dependence of the magnetic specific heat, $C_{mag}(T)$, which was obtained by subtracting $C_p^*(T)$, as extrapolated to $T < 70$ K, from the measured $C_p(T)$ data. There exists a broad peak centered at 30 K, i.e., very close to the Néel temperature inferred from the magnetic-susceptibility measurements. Below $T = 14$ K, we can describe $C_{mag}(T)$ well by

$$C_{mag}(T) = \gamma_{LT}T + \beta T^3 \exp(-\Delta/T), \quad (2)$$

with $\gamma_{LT} = 0.072(2)$ J/K² mole U, $\beta = 8.7 \times 10^{-4}(2)$ J/K⁴ mole U, and $\Delta = 15(2)$ K. The result of this fit is illustrated in the inset of Fig. 7.

In the same way, the $C_p^*(T)$ results for U_2PtGa_3 can be analyzed (Fig. 8) within nearly the same temperature interval as used for the Pd homolog. This yields $\Theta_D = 225(2)$ K and

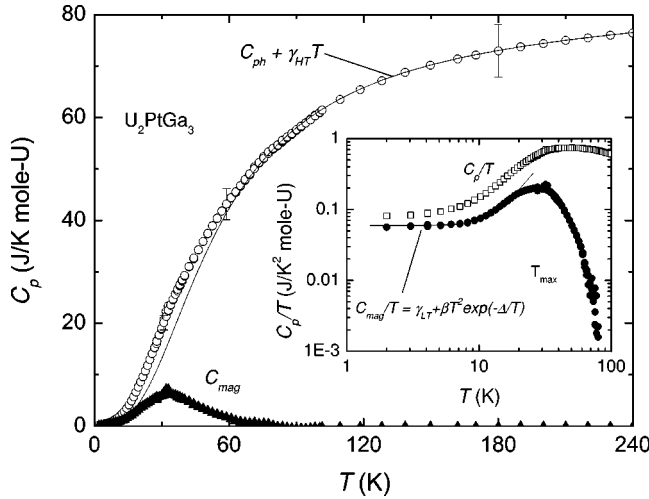


FIG. 8. Measured specific heat of U_2PtGa_3 (open circles), with an accuracy as indicated by the error bars, the sum of both the high-temperature electronic and the phonon contribution (solid line), as well as the magnetic contribution (close triangles), as functions of temperature. Inset: the low-temperature part of the magnetic contribution and the raw C_p data in the C/T vs T representation. The solid line represents a fit to the low-temperature C_{mag} data (see the text).

$\gamma_{HT} = 0.019(2)$ J/K² mole U. By subtracting $C_p^*(T)$ from the $C_p(T)$ data we obtain, according to Eq. (2), $C_{mag}(T)$ with $\gamma_{LT} = 0.061(2)$ J/K² mole U, $\beta = 8.1(2) \cdot 10^{-4}$ J/K⁴ mole U and $\Delta = 18(2)$ K (cf. the inset of Fig. 8). Note that, in contrast to the susceptibility and the MR results, $C_p(T)$ of U_2PtGa_3 does not display any anomaly at $T_m = 80$ K.

We would like to add that the “total” Sommerfeld coefficient $\gamma = \gamma_{HT} + \gamma_{LT}$ as obtained from the above fit procedure, agrees, within the uncertainty margins given, with γ as obtained by plotting the raw data as C_p/T vs T^2 : We find these data of both compounds to be well described by a straight line for $T < 7$ K, yielding $\gamma = C_p/T$ ($T \rightarrow 0$) = 0.092 and 0.079 J/K² mole U for the Pd and Pt compounds, respectively.

The magnetic specific heat $C_{mag}(T)$ also depends linearly on temperature as $T \rightarrow 0$. This might be related to SG freezing as observed in the “random-bond” SG $U_2Rh_2Ge_2$.¹⁶ However, in this case $C_{mag}(T) = \gamma T + DT^k$, where $k = 1.9$, in striking contrast to the $T^3 \exp(-\Delta/T)$ dependence found for our compounds. Therefore, we discard SG freezing as a potential origin for the $\gamma_{LT}T$ term in $C_{mag}(T)$ for the U_2TGa_3 compounds. Instead, we ascribe this term to the Kondo effect that appears to be operating in the presence of AF order, similar to what is well known for canonical Ce-based Kondo-lattice systems like $CeAl_2$.¹⁷ As to the second term on the right-hand side of Eq. (2), this manifests a three-dimensional anisotropic AF magnon spectrum.¹⁸ Note, however, that $C_{mag}(T)$ does not display any discontinuity at the Néel temperature for long-range ordered antiferromagnets. We ascribe the broad maximum of the $C_{mag}(T)$ at $T_{max} \approx T_N$ curve to AF order with a short correlation length. In fact, the long-range order (with infinite correlation length) is most likely to be destroyed by the randomness in the U-U ex-

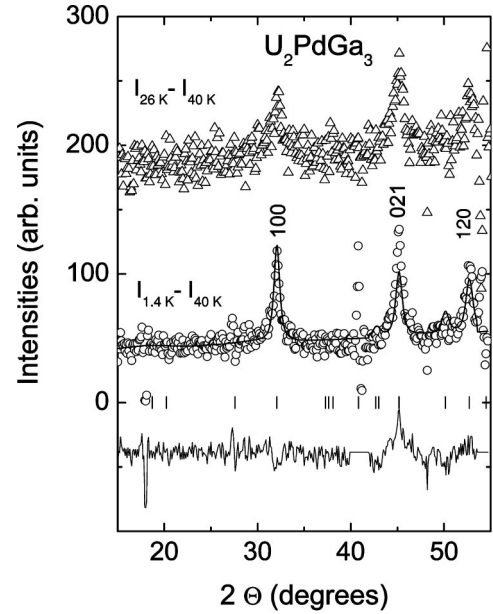


FIG. 9. Difference between the neutron-powder-diffraction patterns of U_2PdGa_3 , taken at low temperatures and at 40 K, respectively.

change interactions. This resembles the case of the crystallographically disordered compound $UAuSn$,¹⁹ for which no specific-heat jump could be resolved, although an AF transition at $T_N \approx 36$ K has been established for this compound by means of NPD (Ref. 20) as well as by ¹¹⁹Sn-Mössbauer studies.²¹ The latter experiments clearly indicated the presence of magnetic inhomogeneities in $UAuSn$. In this context, we recall other examples, e.g., UPd_2In (Ref. 22) and $CeInCu_2$,^{23,24} for which atomic-site disorder causing short-range magnetic order apparently smears out the specific-heat phase-transition anomalies.

Let us finally address the magnetic entropies $S_{mag}(T)$, which for both compounds amount to only a fraction of $R \ln 2$ (namely 68% for U_2PdGa_3 and 65% for U_2PtGa_3) at $T = T_N$. Together with the enhanced γ values, the reduced entropy is characteristic of a magnetically ordered Kondo lattice. This is in qualitative agreement with the assumption of a “Kondo-reduced” U-derived ordered moment, similar to the somewhat reduced Ce-based saturation moments found in Kondo-lattice systems like $CeAl_2$.¹⁷ Of course, the missing magnetic entropy is related to antiferromagnetic short-range correlations, and is released in the paramagnetic state. However, the unavoidable inaccuracy of the specific-heat measurements (several percent) and of the Debye fit to the phonon specific heat in this temperature regime, this contribution cannot be extracted from the data.

E. Magnetic structure

The difference neutron-diffraction patterns $I(1.4 \text{ K}) - I(40 \text{ K})$ and $I(26 \text{ K}) - I(40 \text{ K})$ of U_2PdGa_3 , shown in Fig. 9, give evidence that this compound orders antiferromagnetically at low temperatures. Clearly, the magnetic reflections can be indexed as 100, 021, and 120 within the magnetic unit cell, identical to the crystallographic one. Fur-

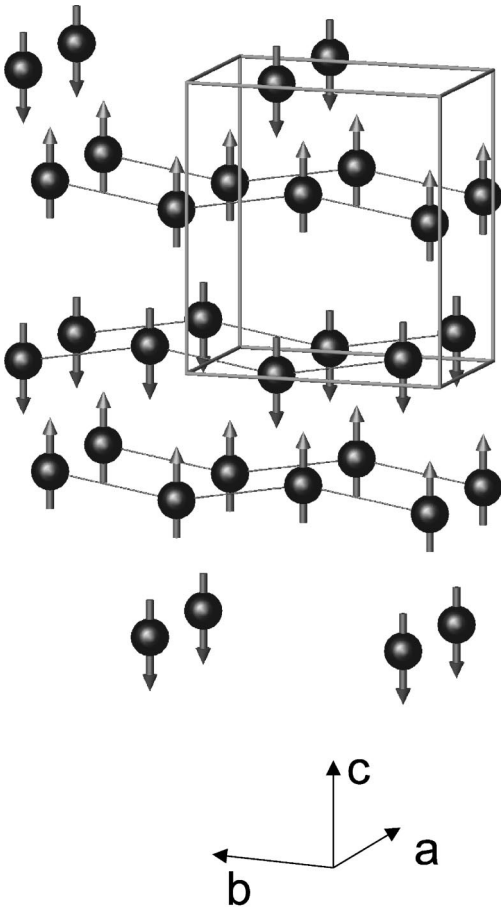


FIG. 10. Model of the magnetic structure of U_2PdGa_3 . Only the uranium atoms with their magnetic moments are shown.

thermore, no signal appears on the reflections (001) or (002) at $2\Theta = 18.15^\circ$ and 36.77° , respectively, indicating that the ordered magnetic moments of uranium, μ_{ord} , is aligned parallel to the c axis.

When we tried the three possible antiferromagnetic models for the arrangement of the signs of the four uranium magnetic moments parallel to the c axis (+ + - -, + - + -, + - - +) the only one compatible with the observed pattern is the spin configuration (+ + - -). In Fig. 10 we display the possible magnetic structure for U_2PdGa_3 . This structure is of a collinear type, in which the pairs of the nearest uranium atoms, U1 and U2 as well as U3 and U4, form two distinct ferromagnetic chains within the bc plane. These chains are coupled antiferromagnetically to each other. In other words, the short U-U distances d_{1-U-U} and d_{3-U-U} are associated with ferromagnetically coupled magnetic moments, while d_{2-U-U} is characterized by antiferromagnetic U-U coupling. Therefore, there is no triangular magnetic structure, which could provide magnetic fluctuations as those observed in SG systems.

Unfortunately, we were not able to refine the uranium magnetic moment with an acceptable agreement factor R_M : Owing to the low intensity of magnetic scattering, we obtain $R_M \approx 20\%$. From the integrated magnetic intensity within the spin configuration (+ + - -), we have estimated the value of ordered uranium magnetic moments to be $0.38(5)\mu_B/\text{U}$.

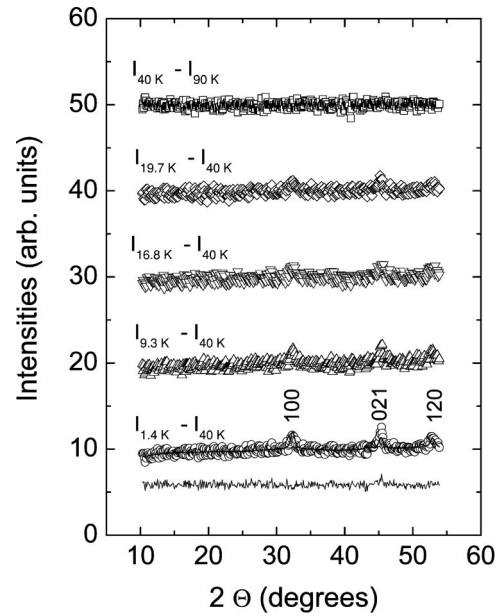


FIG. 11. Difference between the neutron-powder-diffraction patterns of U_2PtGa_3 , taken at low temperatures and at 40 K, respectively. No difference between the patterns collected at 40 K and 90 K could be resolved.

We wish to note that, in addition to the low intensity of the magnetic scattering, we also observed some broadening of the magnetic reflections. A possible explanation for this can be imperfect magnetic order due to, for example, (i) inhomogeneity, (ii) magnetic domains, and (iii) magnetic short-range interactions. The first interpretation requires nuclear Bragg reflections broader than instrumental resolution, which can be clearly discarded (see Fig. 1). To prove the second explanation, single-crystal studies are highly desirable. Here we favor the last explanation, and estimate the magnetic correlation length (MCL) ξ . For U_2PdGa_3 , we obtain ξ of 150 \AA in all (a^* , b^* , and c^*) directions.

As to U_2PtGa_3 , the extra reflections indicating antiferromagnetic order in this compound appear in the NPD patterns taken below 30 K only (Fig. 11). Unlike the magnetic-susceptibility and electric-resistivity measurements, neutron scattering in U_2PtGa_3 could not resolve any features related to magnetic order between 40 and 90 K. We suppose this discrepancy could be due to the very small value of the uranium magnetic moment between $T_N \approx 30 \text{ K}$ and $T_m \approx 80 \text{ K}$. At present we cannot rule out that at T_m the impurity phase detected by nuclear NPD orders ferromagnetically, but is not resolved in the magnetic neutron-diffraction spectra due to its small volume fraction (cf. Sec. II). Like for U_2PdGa_3 (Fig. 9) the low-temperature difference NPD patterns of U_2PtGa_3 (Fig. 11) are all similar to each other. As in the former compound, the magnetic peaks can be indexed as 100, 021, and 120, with a magnetic unit cell being identical to that of U_2PdGa_3 . The magnitude of the ordered magnetic moment at 1.4 K is evaluated to $0.32(5)\mu_B/\text{U}$, practically the same value as found for U_2PdGa_3 . Compared to the moments of the U^{3+} ($3.62\mu_B/\text{U}$) or U^{4+} ($3.58\mu_B/\text{U}$) free ions, the observed values for U_2PdGa_3 and U_2PtGa_3 are

strongly reduced. This, again, is in qualitative agreement with the assumption of a Kondo effect being operative in an antiferromagnetically ordered state.

The MCL value for U_2PtGa_3 was found to be $\xi = 120 \text{ \AA}$, i.e., of similar size as for the Pd homolog. The MCL of the two compounds correspond to about 20 unit-cell dimensions along the b and c axes, and about 40 unit-cell dimensions along the a axis. Therefore, the MCL is longer than reported for the SG compound URh_2Ge_2 ,¹⁶ for which ξ amounts to 45–75 \AA only. However, the MCL is substantially shorter than for the antiferromagnets URu_2Si_2 (Refs. 25 and 26) and UPt_3 .^{27,28} In fact, these latter compounds have MCL's of about 200–500 \AA . We should mention here that both URu_2Si_2 and UPt_3 become heavy-fermion superconductors well below their respectively Néel temperature. Furthermore, their ordered U moments are extremely small, i.e., of order $10^{-2} \mu_B$.

Concerning the observed magnetic structure of U_2PdGa_3 and U_2PtGa_3 , we note that this structure is very similar to that of $UAuGa$.²⁹ This compound adopts the same orthorhombic $CeCu_2$ -type crystal structure, and belongs to the class of classical antiferromagnets, characterized by a collinear magnetic structure, in which the U moments are oriented parallel to the c axis of the orthorhombic crystal structure.

IV. CONCLUSION

We have presented magnetic-susceptibility, electrical-resistivity, magnetoresistance and specific-heat measurements of U_2PdGa_3 and U_2PtGa_3 , in connection with neutron-powder-diffraction experiments. We have confirmed that these compounds crystallize in an orthorhombic $CeCu_2$ -type structure. We have observed a number of features that are consistent with the presence of Kondo-type interactions.

Therefore, the magnetic properties of U_2PdGa_3 and U_2PtGa_3 have to be discussed in terms of an interplay between Kondo and exchange interactions. We suppose that the latter interactions, though considerably weakened by the Kondo effect, are still strong enough to form antiferromagnetic order, but with rather short correlation lengths due to the presence of atomic-site disorder: Various electronic environments around the magnetic U atoms modify the magnetic indirect exchange interactions. The structural disorder may, thus, in fact be the reason for the short magnetic correlation lengths observed in the two compounds. In summary, the combined effects of direct and indirect exchange interactions, on the one hand, as well as of Kondo interactions and randomness on the other hand, appear to govern the magnetic properties of U_2PdGa_3 and U_2PtGa_3 .

Finally, we would like to recall that similar scenarios have been assumed for some non-Fermi-liquid (NFL) systems,^{30,31} showing either a distribution of Kondo temperatures (including $T_K = 0$) (Refs. 32–34) or structural disorder in the paramagnetic state very close to a quantum critical point (QCP).³⁵ Future investigations of the U_2TGa_3 systems should shed more light on the problem of such disordered magnets in the vicinity of a QCP. In order to suppress AF order, we plan to apply hydrostatic and/or chemical pressure. From the NFL scaling behaviors established near the potential QCP of these two compounds, we expect a deeper insight into the interplay between structural disorder and magnetic interactions.

ACKNOWLEDGMENTS

One of the authors (V.H.T.) thanks Professor R. Troć and Dr. Z. Hossain for valuable discussions.

-
- ¹V. H. Tran, *J. Phys.: Condens. Matter* **8**, 6267 (1996).
²A. Schröder, M. F. Collins, C. V. Stager, J. D. Garrett, J. E. Greedan, and Z. Tun, *J. Magn. Magn. Mater.* **140-144**, 1407 (1995).
³B. Chevalier, R. Pöttgen, B. Darriet, P. Gravereau, and J. Etourneau, *J. Alloys Compd.* **233**, 150 (1996).
⁴D. Kaczorowski and H. Noël, *J. Phys.: Condens. Matter* **5**, 9185 (1993).
⁵D. X. Li, Y. Shiokawa, Y. Homma, A. Uesawa, and T. Suzuki, *J. Magn. Magn. Mater.* **176**, 261 (1997).
⁶D. X. Li, Y. Shiokawa, Y. Homma, A. Uesawa, A. Dönni, T. Suzuki, Y. Haga, E. Yamamoto, T. Honma, and Y. Onuki, *Phys. Rev. B* **57**, 7434 (1998).
⁷D. X. Li, A. Dönni, Y. Kimura, Y. Shiokawa, Y. Homma, Y. Haga, E. Yamamoto, T. Honma, and Y. Onuki, *J. Phys.: Condens. Matter* **11**, 8263 (1999).
⁸J. Rodriguez-Carvajal, *Physica B* **192**, 55 (1993).
⁹V. F. Sears, *Neutron News* **3**, 26 (1992).
¹⁰A. J. Freeman, J. P. Desclaux, G. H. Lander, and J. Faber, Jr., *Phys. Rev. B* **13**, 1168 (1976).
¹¹K. Binder and H. P. Young, *Rev. Mod. Phys.* **58**, 801 (1986).
¹²J. A. Mydosh, *Spin Glasses: An Experimental Introduction* (Taylor and Francis, London, 1993).
¹³S. Majumdar, E. V. Sampathkumaran, P. L. Paulose, H. Bitterlich, W. Löser, and G. Behr, *Phys. Rev. B* **62**, 14 207 (2000).
¹⁴P. Schlottmann, *Z. Phys. B: Condens. Matter* **51**, 223 (1983).
¹⁵A. K. Nigam and A. K. Majumdar, *Phys. Rev. B* **27**, 495 (1983).
¹⁶S. Süllow, G. J. Nieuwenhuys, A. A. Menovsky, J. A. Mydosh, S. A. M. Mentink, T. E. Mason, and W. J. L. Buyers, *Phys. Rev. Lett.* **78**, 354 (1997).
¹⁷F. Steglich, C. D. Bredl, M. Loewenhaupt, and K. D. Schotte, *J. Phys. (Paris)* **40**, 301 (1979).
¹⁸A. R. Mackintosh, *Phys. Lett.* **4**, 140 (1963).
¹⁹F. R. De Boer, E. Brück, H. Nakotte, A. V. Andreev, V. Sechovsky, L. Havela, P. Nozar, C. J. M. Denissen, K. H. J. Buschow, B. Vaziri, M. Meissner, H. Maletta, and P. Rogl, *Physica B* **176**, 275 (1992).
²⁰R. A. Robinson, J. W. Lynn, V. Nunez, K. H. J. Buschow, H. Nakotte, and A. C. Lawson, *Phys. Rev. B* **47**, 5090 (1993).
²¹R. Kruk, R. Kmiec, K. Łątka, K. Tomala, R. Troć, and V. H. Tran, *J. Alloys Compd.* **232**, L8 (1996).
²²T. Takabatake, H. Kawanaka, H. Fujii, Y. Yamaguchi, J. Sakurai,

- Y. Aoki, and T. Fujita, *J. Phys. Soc. Jpn.* **58**, 1918 (1989).
- ²³R. Lahiouel, J. Pierre, E. Siaud, R. M. Galera, M. J. Besnus, J. P. Kappler, and A. M. Murani, *Z. Phys. B: Condens. Matter* **67**, 185 (1987).
- ²⁴Y. Onuki, T. Yamazaki, A. Kobori, T. Omi, T. Komatsubara, S. Takayanagi, H. Kato, and N. Wada, *J. Phys. Soc. Jpn.* **56**, 4251 (1987).
- ²⁵C. Broholm, J. K. Kjems, W. J. L. Buyers, P. Matthews, T. T. M. Palstra, A. A. Menovsky, and J. A. Mydosh, *Phys. Rev. Lett.* **58**, 1467 (1987).
- ²⁶B. Fåk, C. Vettier, J. Flouquet, F. Bourdarot, S. Raymond, A. Vernière, P. Lejay, Ph. Boutrouille, N. R. Bernhoeft, S. T. Bramwell, R. A. Fisher, and N. E. Phillips, *J. Magn. Magn. Mater.* **154**, 339 (1996).
- ²⁷G. Aeppli, E. Bucher, C. Broholm, J. K. Kjems, J. Baumann, and J. Hufnagl, *Phys. Rev. Lett.* **60**, 615 (1988).
- ²⁸Y. Koike, N. Metoki, N. Kimura, E. Yamamoto, Y. Haga, Y. Onuki, and K. Maezawa, *J. Phys. Soc. Jpn.* **67**, 1142 (1998).
- ²⁹V. H. Tran, F. Bourée, G. André, and R. Troć, *Solid State Commun.* **98**, 111 (1996).
- ³⁰B. Andraka and G. R. Stewart, *Phys. Rev. B* **47**, 3208 (1993).
- ³¹R. Chau and M. B. Maple, *J. Phys.: Condens. Matter* **8**, 9939 (1996).
- ³²O. O. Bernal, D. E. MacLaughlin, H. G. Lukefahr, and B. Andraka, *Phys. Rev. Lett.* **75**, 2023 (1995).
- ³³E. Miranda, V. Dobrosavljević, and G. Kotliar, *J. Phys.: Condens. Matter* **8**, 9871 (1996).
- ³⁴E. Miranda and V. Dobrosavljević, *Physica B* **259-261**, 359 (1999).
- ³⁵A. H. Castro Neto, G. Castilla, and B. A. Jones, *Phys. Rev. Lett.* **81**, 3531 (1998).